

SUPPORTING INFORMATION FOR: Defining single molecular forces required for Notch activation using nano yoyo

Farhan Chowdhury^{1,2,3*}, Isaac T. S. Li^{2,4*}, Thuy T. M. Ngo², Benjamin J. Leslie⁵, Byoung Choul Kim^{5,6},
Joshua E. Sokoloski⁷, Elizabeth Weiland⁷, Xuefeng Wang^{2,8}, Yann R. Chemla², Timothy M. Lohman⁷,
Taekjip Ha^{2,5,6,†}

¹*Department of Mechanical Engineering and Energy Processes, Southern Illinois University Carbondale, Carbondale, IL 62901, U.S.A.;* ²*Department of Physics and Center for Physics of Living Cells, University of Illinois at Urbana-Champaign, Urbana, IL 61801, U.S.A.;* ³*Carl R. Woese Institute for Genomic Biology, University of Illinois at Urbana-Champaign, Urbana, IL 61801, U.S.A.;* ⁴*Department of Chemistry, University of British Columbia Okanagan, Kelowna, British Columbia, V1V 1V7, Canada;* ⁵*Howard Hughes Medical Institute, Johns Hopkins University, Baltimore, MD, U.S.A.;* ⁶*Departments of Biophysics and Biophysical Chemistry, Biophysics and Biomedical Engineering, Johns Hopkins University, Baltimore, MD, U.S.A.;* ⁷*Department of Biochemistry and Molecular Biophysics, Washington University in St. Louis, St. Louis, MO 63110, U.S.A.;* ⁸*Department of Physics and Astronomy, Iowa State University, Ames, IA 50011, U.S.A.;*

* These authors contributed equally to this work

†Correspondence: T.H. (Email: tjha@jhu.edu, Fax: +1 217-144-7187)

This PDF file includes

- **Materials and Methods [Pg. S2-S8]**
- **Supporting Figures [Pg. S9-S18]**
- **References [Pg. S19-S20]**

MATERIALS AND METHODS

Cell culture and treatments

Transgenic notch reporter CHO-K1 cells were cultured as before¹. Briefly, they were cultured in alpha MEM Earl Salts (Irvine Scientific #9144) supplemented with Tet System approved 10% FBS (Clontech), L-Glutamine (Invitrogen), and Pen/Strep (Invitrogen). Culture medium also contained 10μg/ml Blastocidin, 400μg/ml Zeocin, 600μg/ml Geneticin. Cells were treated with DAPT (Sigma) in varying concentrations as indicated.

DNA constructs sequence

All DNA constructs were purchased from Integrated DNA Technologies. For the force spectroscopy measurements, as shown in Supplementary Fig. 1, the sequence of the top construct on the stationary bead is 5'/AGG TCG CCG CCC GGG TGG TCG CTG CGG GCC TTT TT-3' named as (dT)₆₅. The bottom construct sequence for (dT)₆₅ is 5'-/GGC CCG CAG CGA CCA CCC-3'. For cell culture experiments, sequence of the top construct is 5'/ GGG TGG TCG CTG CGG GCC TTT TT-3' while the bottom ssDNA construct sequence is 5'-Cy3/GGC CCG CAG CGA CCA CCC- /3ThioMC3-D/-3'.

Creation of SSB-LT-Drl with Biotinylation Site/AviTag

The AviTag² sequence GLNDIFEAQKIEWHE was added to the C terminus of SSB-LT-Drl³ by first adding the AviTag sequence to SSB LD Drl and then cloning the second dimer upstream of the LD Drl to create SSB-LT-Drl-AviTag.

A PCR product of SSB-LD-Drl-AviTag was created using a forward primer in the T7 promoter region - GCG AAA TTA ATA CGA CTC ACT ATA GGG G and a reverse primer containing the AviTag sequence and a BamHI restriction site - GAA TTC GGA TCC TTA CTC GTG CCA CTC GAT CTT CTG GGC TTC GAA GAT GTC GTT TAG GCC GAA CGG AAT GTC ATC ATC AAA GTC C using SSB LD Drl as template. The creation of SSB-LD-Drl has been described previously³, but briefly, the SSB LD Drl construct was cloned into a pET21a vector using the NdeI and BamHI restriction sites. The SSB operon was then cloned upstream of the start site using the XbaI and NdeI sites.

The resulting SSB LD Drl AviTag PCR product was purified with a QIAquick PCR Purification Kit (Qiagen, Cat. No. 28106) and both this PCR product and pET21a vector (Novagen) were digested with XbaI and BamHI, purified again, ligated with T4 DNA ligase (New England Biolabs) and used to transform XL-10 Gold cells (Stratagene). Colonies were screened for the correct insert size and then sequenced to confirm the creation of SSB-LD-Drl-AviTag with no mutations.

To generate SSB-LT-Drl-AviTag from SSB LD Drl AviTag, a PCR product containing the SSB LD Drl flanked by NdeI sites was created using a forward primer in the SSB operon CGC GCG TTT ACA CTT ATT CAG AAC G, and the reverse primer GCC ACC TGC CGG AGC GCC ACC ACC CTG ACG ACC ACC CAT ATG GCT AGC CAG CAT CTG C on a SSB LD Drl vector intermediate in the creation of the original of LT and LD Drl constructs. The resulting PCR product was PCR purified as above. This product and SSB-LT-Drl-AviTag were digested with NdeI, purified, ligated, and used to transform XL-10 Gold cells. Colonies showing the correct size insert were sequenced to confirm no mutations. DNA from a good clone (pEW406, ampicillin

resistant) was then transformed into BL21 DE3 Gold cells (Stratagene) and expression of SSB-LT-Drl-AviTag protein confirmed.

Purification and Characterization of SSB-LT-Drl-AviTag

A 10 mL culture of pEW406 cells were grown overnight starting from a single colony. This was used to inoculate 1 liter of Terrific Broth⁴ containing 50 µg/mL ampicillin. Cells were grown at 37°C with 300 rpm shaking in Fernbach flasks. At OD₆₀₀ = 0.8, SSB-LT-DrL-AviTag overexpression was induced by the addition of IPTG to a final concentration of 0.5 mM. At the same time, biotin (dissolved in 10 mM bicine buffer pH 8.3) was added to a final concentration of 50 µM. The cells were incubated with shaking at 37°C for three hours post induction. Cells were harvested by centrifugation and stored at -80°C.

SSB-LT-Drl-AviTag protein was purified as reported previously³. The extent of biotinylation of the AviTag site was 53% as determined via a HABA (ThermoScientific) assay⁵. A sedimentation velocity analytical ultracentrifugation experiment of the protein showed a single species of S-value 3.4 and estimated molecular weight of 65 kDa consistent with monomeric SSB-LT-DrL-AviTag (SFX A). Titration of SSB-LT-Drl-AviTag with (dT)₇₀ monitored by tryptophan fluorescence quenching⁶ showed formation of a high affinity complex with 1:1 stoichiometry (SFX B). A single molecule TIRF assay was performed by binding SSB-LT-DrL-AviTag to a 25:1 biotinylated PEG surface via a biotin-Neuravidin-biotin linkage⁷ followed by addition of 5' Cy3-labeled 40 deoxynucleotide mixed sequence ssDNA and subsequent washing with a buffer of 10 mM Tris-HCl pH 8.1 and 200 mM NaCl. Isolated Cy3 fluorescence spots appeared in the field indicating that immobilized SSB-LT-Drl-AviTag maintains its DNA binding activity.

Optical tweezer experiment

All optical tweezer experiments were performed in a buffer containing 100 mM Tris-HCl (pH 7.6), 50 mM Na⁺ and 5mM Mg²⁺) at room temperature. Protocatechuic acid (PCA, 37580 ALDRICH)/protocatechuate-3,4-dioxygenase (PCD, P8279 SIGMA) oxygen scavenger system was used to increase tether lifetime⁸; Streptavidin and protein G beads were purchased from Spherotech. Protein G beads were subsequently functionalized by anti-digoxigenin following established protocols. btSSB:(dT)₆₅ was incubated with streptavidin bead while the COS-3kbp handle was incubated with anti-digoxigenin bead for 1 hour at room temperature. Custom flow chamber as previously described was used for all optical tweezer experiments where one trap holds the streptavidin bead with btSSB:(dT)₆₅ and the other other trap holds the anti-digoxigenin bead with the COS-3kbp handle. The stiffness of both traps were calibrated by measuring the thermal spectra of the bead motion, yielding a typical value of 0.5 pN/nm. The beads were brought close but not touching to form single tethers. The contour length and stiffness of the resulting tether matches those of a single DNA tether.

Fabrication of DLL1- LTGT

The assembly of btSSB:ssDNA LTGT is described in the flow diagram as shown in Supplementary Fig. 3. Protein G was conjugated to the 3' end of 18 nucleotide ssDNA via hetero-bifunctional crosslinker (Sulfo-SMCC, Thermo Fisher Scientific Inc.). Sulfo-SMCC has maleimide and NHS ester groups on two ends which react with the –SH group on the –SH modified ssDNA and amine on Protein G. 18 nt ssDNA- Protein G and (dT)₆₅ ssDNA with complimentary 18 nt sequence were annealed in annealing buffer overnight at 4° C. DLL1-Fc (gift from I. D. Bernstein) were conjugated to Protein G. These intermediate complexes were then incubated with biotinylated SSB

at 1:1 molar ratio making the final complex of btSSB: ssDNA LTGT. Glass bottom cell culture dishes were incubated with biotin labeled BSA (Sigma) and fibronectin (Sigma) for 30 min in room temperature. Following the incubation, the glass surfaces were washed with PBS and further incubated with NeutrAvidin (Thermo Fisher Scientific) for 10 min at room temperature. It was washed again with PBS and incubated with different concentration of btSSB: ssDNA LTGT.

Fluorescence microscopy and image analysis

A Zeiss Axiovert 200M inverted fluorescence microscope (Zeiss, Germany), equipped with a cooled EMCCD camera (Photometrics, Cascade 512), Xcite illuminator, motorized stage, and 20x objective, YFP filter cube set was used for fluorescence imaging. Also, a Zeiss LSM 710 laser scanning confocal microscope was used to monitor time dependent rupture of DLL1-LTGT from the surface. All live cell imaging were performed in low serum (1%) cell culture medium at 37° C. NIH ImageJ was used for fluorescence image quantification.

For quantification of LTGT rupture in Fig 4, we utilized the following formula:

$$Rupture \% = \frac{(Background - rupture)}{(background - baseline)} \times 100 \quad (1)$$

Cell boundary was determined by Sobel edge detection method from phase-contrast images. The brighter nuclei of cells were excluded from rupture analysis. The area between nuclei and cell boundary defines the region of rupture analysis. The immediate region outside the cell boundary (red) was used as background. Histogram of each region was shown and the fit to the histogram was used to calculate percentage of rupture. The baseline value was obtained from non-fluorescent images and were subtracted from both ruptured and background regions.

Gene array scanning

We used a fluorescence technique to visualize surface density of DLL1-LTGTs incubated under 37° C. The DLL1-LTGT contains a Cy3 fluorophore. A gene array scanner (Genepix 4000B Microarray scanner, Molecular Devices LLC) with 100% power and EM gain of 500 was utilized to acquire fluorescence images of surface immobilized with LTGTs at different concentrations.

Notes

There might be a concern that the tension tolerance of the nano-yoyo probes might shift since the conditions such as temperature and salt concentrations differ between calibration and live cell experiments. All our trap calibration was done at room temperature while cell experiments were carried out at 37° C. We could not perform trap calibration experiments at 37° C due to technical limitations. We acknowledge this caveat that proteins may rupture at lower forces at higher temperatures, thus may lower the tension tolerance of LTGTs compared to the *in vitro* calibration value. However, the difference in salt concentration, particularly Na⁺ and Mg⁺² may not have a profound effect because of the following reasons. The salt concentration primarily affects the mode of interaction between SSB and ssDNA. We have shown in the past that if the salt concentration is high enough above a certain threshold, ssDNA-SSB will have a fully wrapped mode⁹. In our earlier work⁹, we demonstrated that about 100mM Na⁺ with 10 nM SSB concentration (which is our cell experimental condition) majority of them favored fully wrapped mode. Even 10 mM Na⁺ was enough to have a fully wrapped mode for low SSB concentration. Therefore, we anticipate to achieve a fully wrapped mode during both trap experiment and cell culture experiment that had Na⁺ concentration of at least 50 mM. In addition, the Mg⁺² ion concentration in trap experiment and cell culture medium were sufficiently high, to be 5 mM and ~1 mM respectively, so that the

fully wrapped mode was even more favored. In an earlier work¹⁰, when we applied forces from two ends of the DNA (although a different loading configuration than LTGTs), we did not observe a significant shift in dominant ssDNA-SSB dissociation force peak (~9-10 pN) when 5mM Mg^{+2} was added to the buffer. This suggests that difference in Mg^{+2} between trap experiment and cell culture should not have significant influence that can cause a major shift in LTGT tension tolerance.

SUPPORTING FIGURES

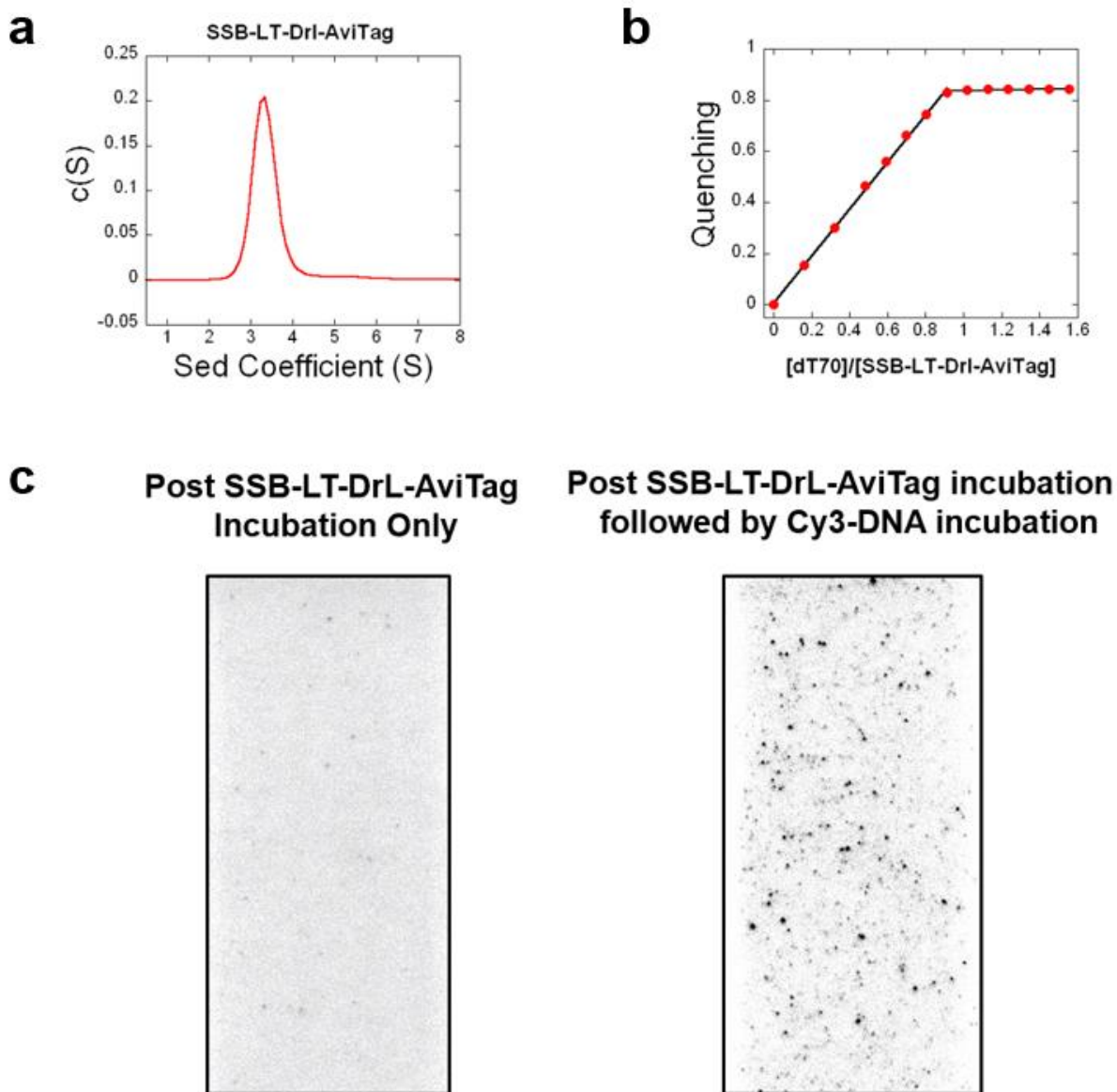


Figure S1. Characterization of SSB-LT-DrL-AviTag. **(a)** Sedimentation velocity analysis at 42,000 rpm shows a single predominant species. The estimated molecular weight calculated from this data was 65 kDa, within 5% of the 62 kDa calculated previously with sedimentation equilibrium analysis³. A small, broad peak around 5.5S may represent a small amount of SSB-

LT-Drl-AviTag dimers. Conditions: 50 mM Tris pH 8.1, 300 mM NaCl, 1 mM Na₂EDTA, 5% (v/v) glycerol, 25°C. **(b)** Titration of 19.1 μM (dT)₇₀ into SSB-LT-Drl-AviTag with an initial concentration of 89 nM, monitored by intrinsic tryptophan fluorescence quenching. Maximum quenching (Q=0.84) was reached at a DNA:SSB ratio of 0.91. Conditions: 50 mM Tris pH 8.1, 300 mM NaCl, 1 mM Na₂EDTA, 5% (v/v) glycerol, 25°C. **(c)** *Left image:* Incubation of 200 pM SSB-LT-Drl-AviTag with a Neutravidin-treated biotinylated PEG surface revealed no significant accumulation of fluorescent spots beyond pre-existing background surface contaminants. *Right image:* Addition of 370 pM 5' Cy3 d(CCA TGG CTC CTG AGC TAG CTG CAG TAG CCT ATG CTC CAG) DNA to the same post-SSB-LT-Drl-AviTag surface reveals accumulation of fluorescent signals detected in the TIRF illumination volume that persist with washing indicating DNA bound to immobilized SSB-LT-Drl-AviTag. Conditions: 10 mM Tris-HCl pH 8.1, 200 mM NaCl, 0.1 mM Na₂EDTA, 3 mM Trolox, 0.1 mg/mL BSA, 0.5% dextrose, and a glucose oxidase/catalase oxygen-scavenging enzyme mix. T = 25°C.

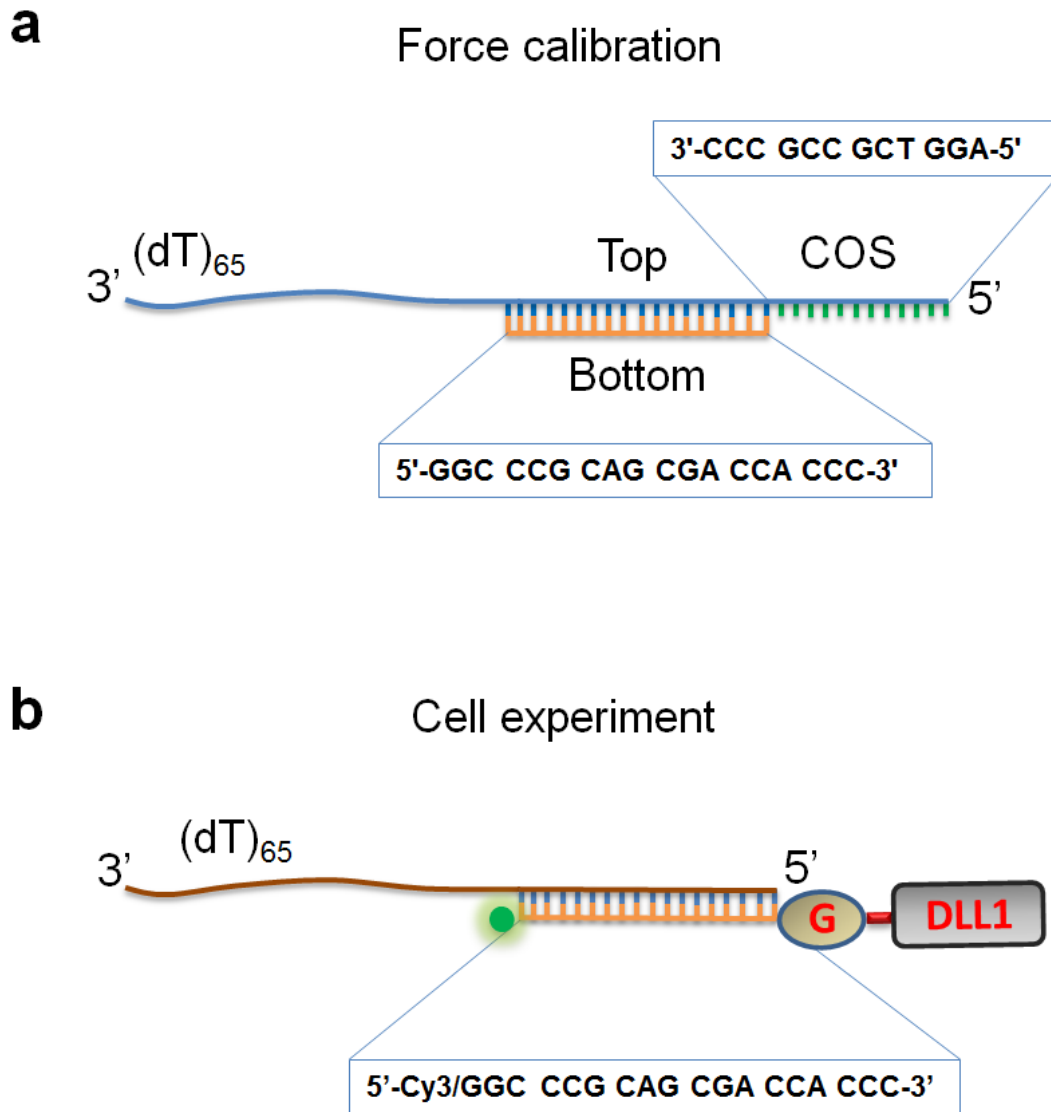


Figure S2. (a-b) A schematic showing similarity of btSSB: ssDNA LTGT during force calibration and cell experiments.

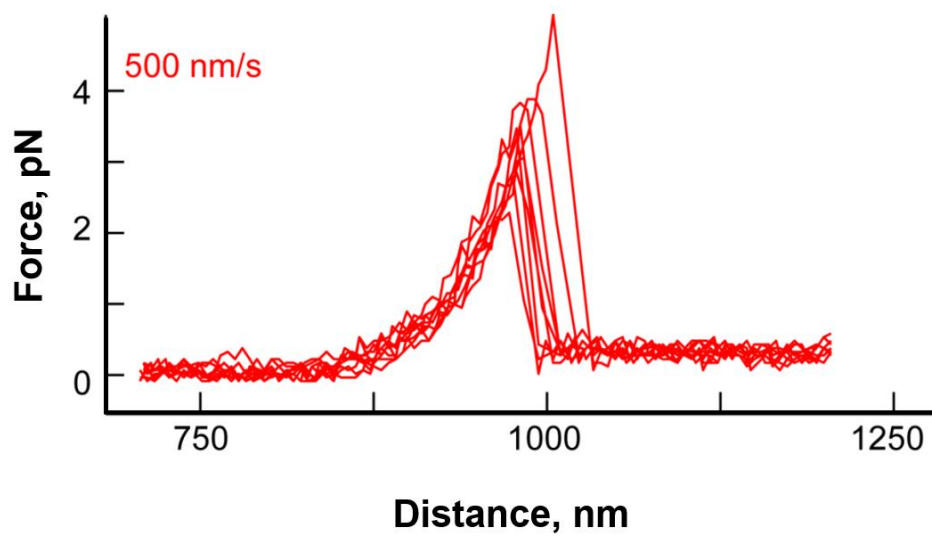


Figure S3. Typical force vs. distance traces obtained from high-resolution optical tweezers.

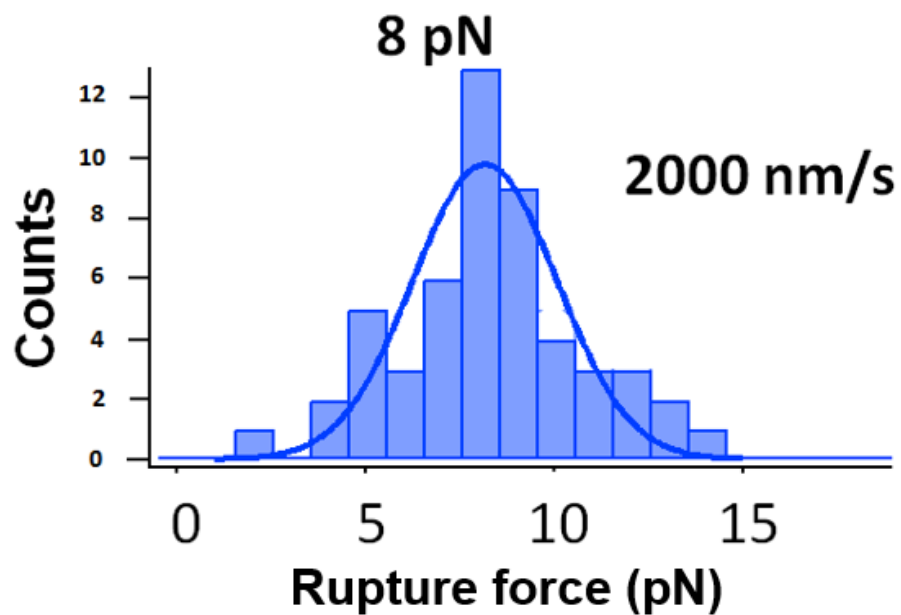


Figure S4. ssDNA rupture from surface immobilized SSB is pulling rate dependent. When the pulling rate was increased to 2000 nm/s, ssDNA rupture force was increased to 8 pN.

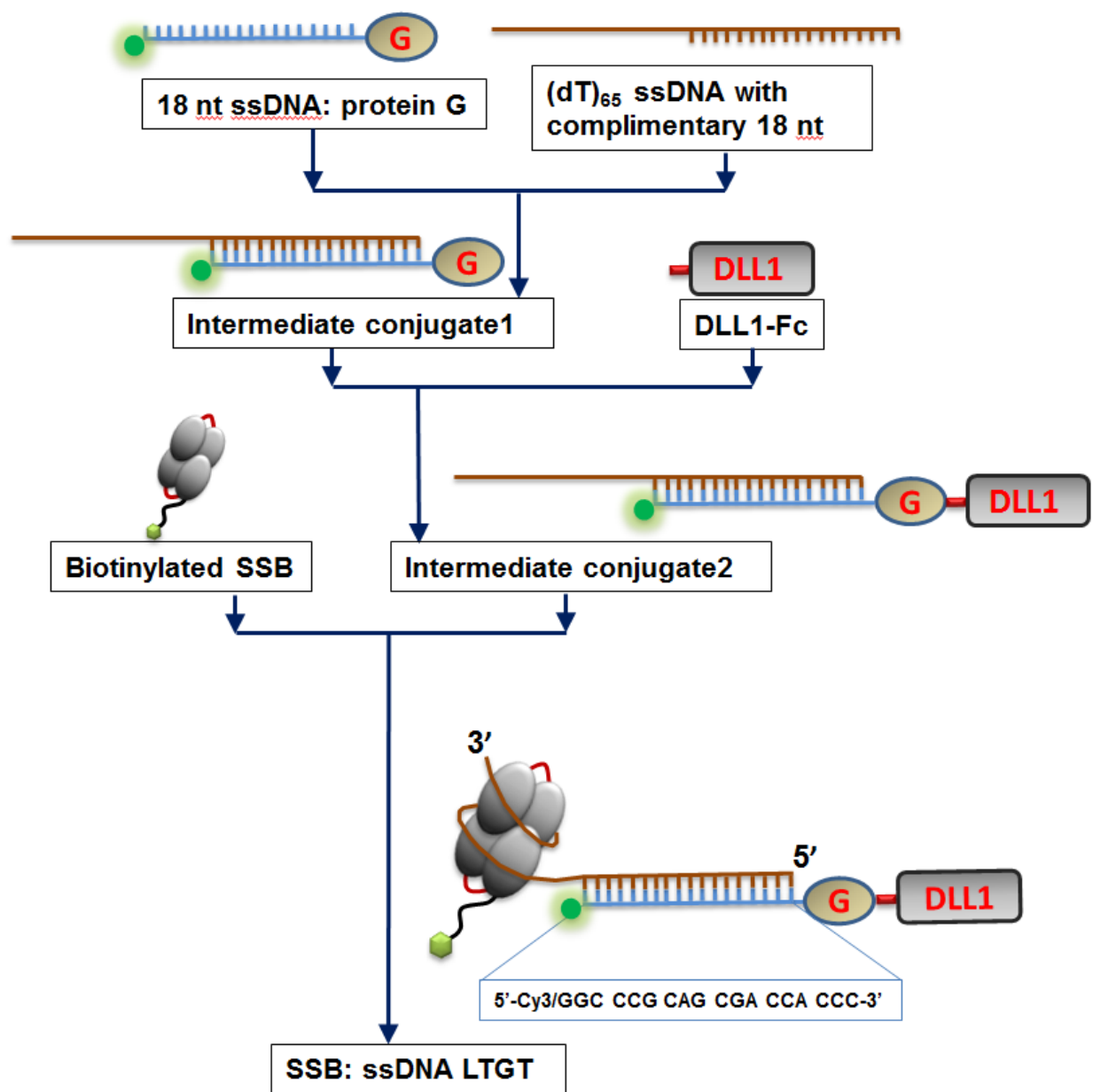


Figure S5. A flow diagram for fabrication of btSSB: ssDNA LTGT.

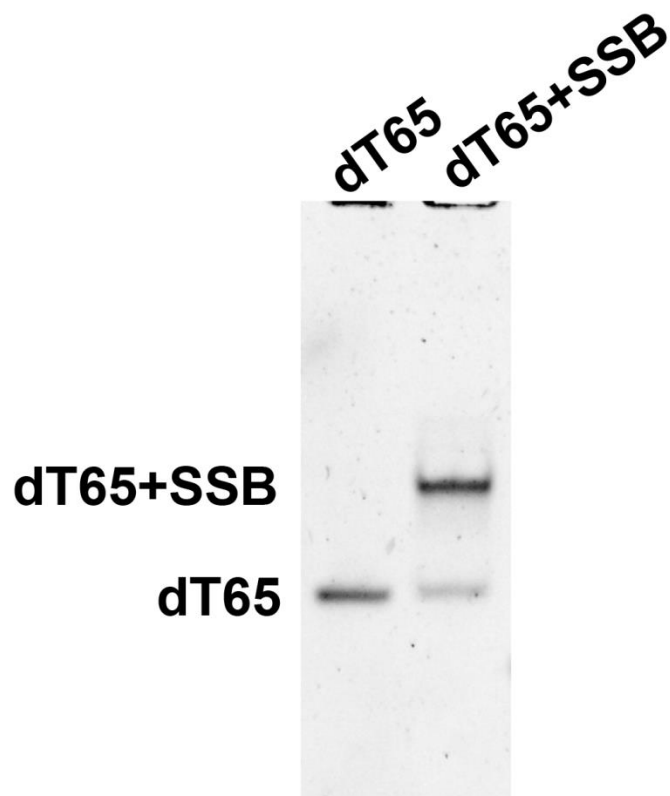


Figure S6. Electrophoretic mobility shift assay shows that when $(dT)_{65}$ constructs were mixed with SSB at 1:1 molar ratio only single bands were observed confirming the formation of a stable btSSB: DNA complexes.

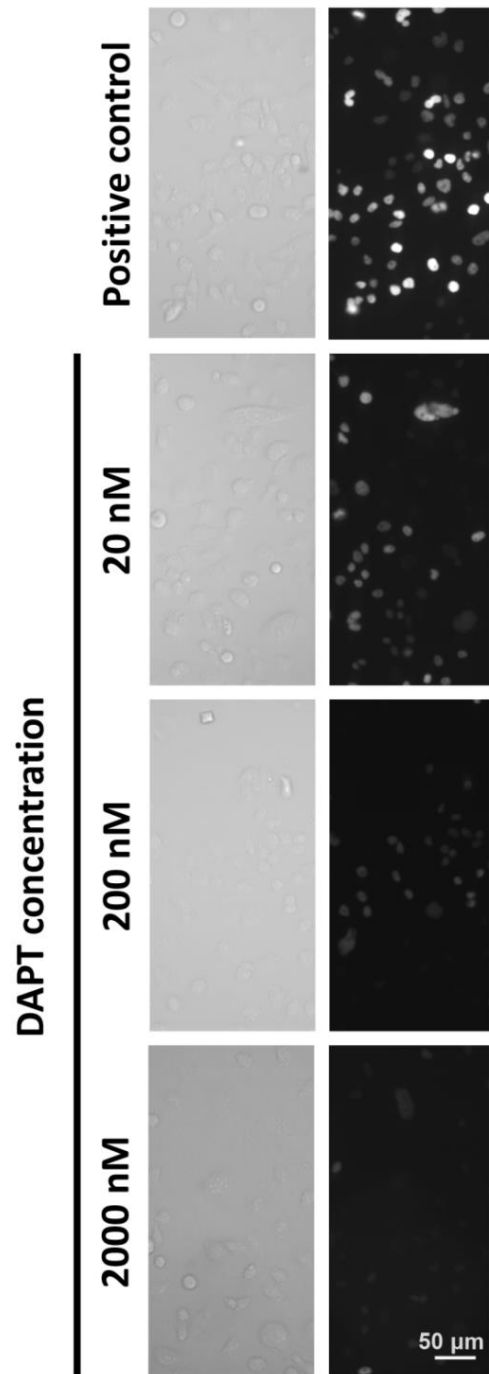


Figure S7. Inhibition of protease for cleavage of Notch receptors inhibits Notch activation. When cells are treated with DAPT^{11, 12}, a chemical known to inhibit γ -Secretase, Notch activation reduces in a dose dependent manner.

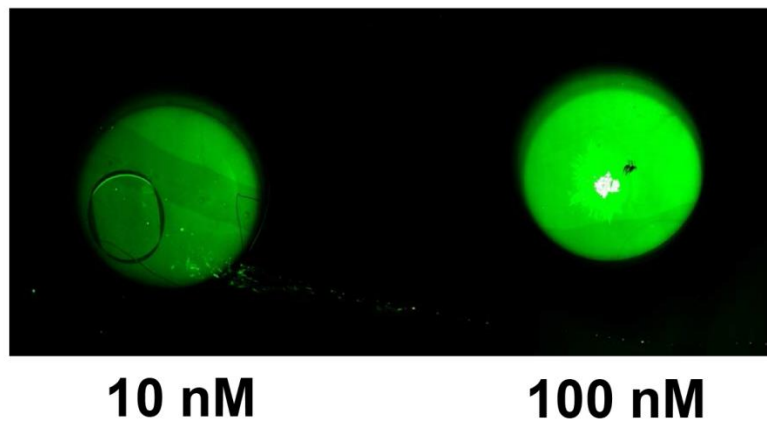


Figure S8. A gene array scan shows surface immobilized LTGT density on the surface when incubated at 37° C at 10 nM and 100 nM concentrations.

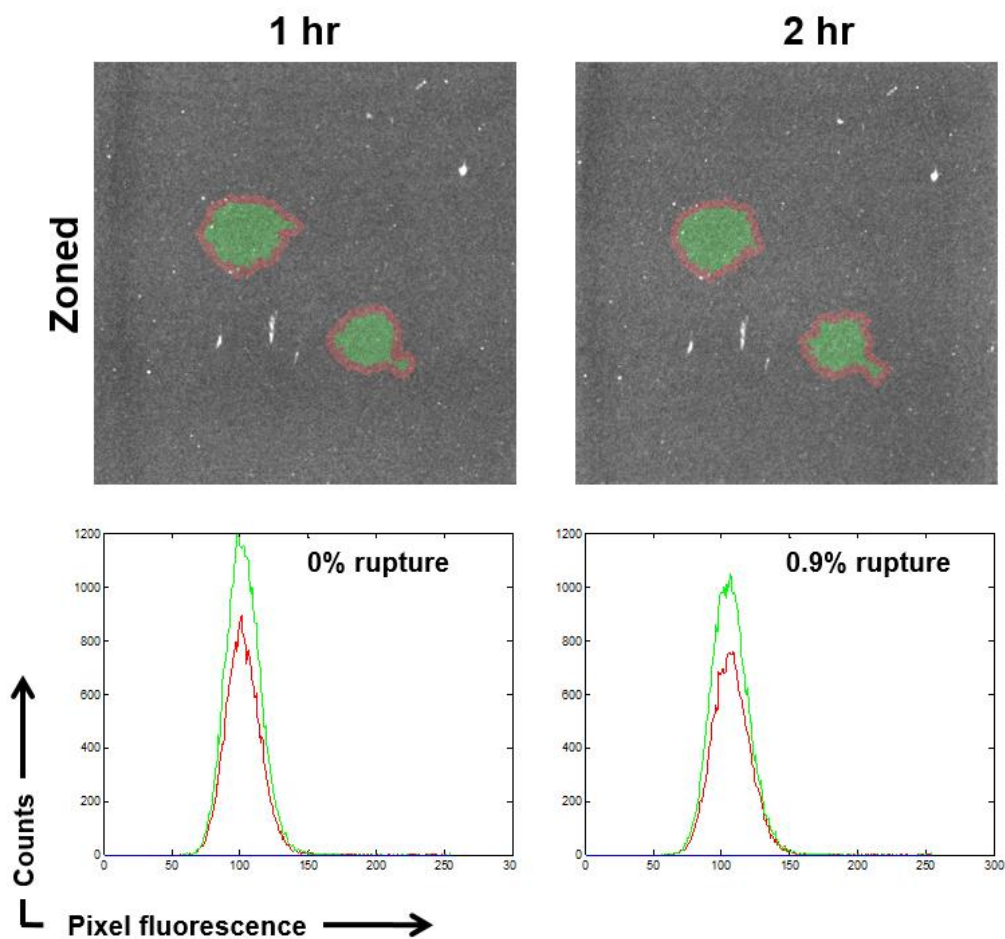


Figure S9. No significant fluorescence loss is observed on 12 pN TGT surface over time. Red, and green regions indicate background and rupture regions respectively. Both ruptured and background regions were baseline corrected (obtained from non-fluorescent images). Histograms of each region were plotted and rupture percentage was calculated from the fit to the histogram.

References

1. Wang, X.; Ha, T. *Science* **2013**, 340, 991-4.
2. Ashraf, S. S.; Benson, R. E.; Payne, E. S.; Halbleib, C. M.; Gron, H. *Protein Expr Purif* **2004**, 33, 238-45.
3. Antony, E.; Weiland, E.; Yuan, Q.; Manhart, C. M.; Nguyen, B.; Kozlov, A. G.; McHenry, C. S.; Lohman, T. M. *J Mol Biol* **2013**, 425, 4802-19.
4. Tartoff, K.; Hobbs, C. *Bethesda Research Laboratories Focus* **1987**, 9.
5. Green, N. M., *Methods in Enzymology*. Academic Press: New York, 1970; Vol. 18A, 418-424.
6. Kozlov, A. G.; Galletto, R.; Lohman, T. M. *Methods Mol Biol* **2012**, 922, 55-83.
7. Roy, R.; Hohng, S.; Ha, T. *Nat Methods* **2008**, 5, 507-16.
8. Aitken, C. E.; Marshall, R. A.; Puglisi, J. D. *Biophys J* **2008**, 94, 1826-35.
9. Roy, R.; Kozlov, A. G.; Lohman, T. M.; Ha, T. *J Mol Biol* **2007**, 369, 1244-57.
10. Zhou, R.; Kozlov, A. G.; Roy, R.; Zhang, J.; Korolev, S.; Lohman, T. M.; Ha, T. *Cell* **2011**, 146, 222-32.
11. Dovey, H. F.; John, V.; Anderson, J. P.; Chen, L. Z.; de Saint Andrieu, P.; Fang, L. Y.; Freedman, S. B.; Folmer, B.; Goldbach, E.; Holsztynska, E. J.; Hu, K. L.; Johnson-Wood, K. L.; Kennedy, S. L.; Kholodenko, D.; Knops, J. E.; Latimer, L. H.; Lee, M.; Liao, Z.; Lieberburg, I. M.; Motter, R. N.; Mutter, L. C.; Nietz, J.; Quinn, K. P.; Sacchi, K. L.; Seubert, P. A.; Shopp, G. M.; Thorsett, E. D.; Tung, J. S.; Wu, J.; Yang, S.; Yin, C. T.; Schenk, D. B.; May, P. C.; Altstiel, L. D.; Bender, M. H.; Boggs, L. N.; Britton, T. C.; Clemens, J. C.; Czilli, D. L.; Dieckman-McGinty, D. K.; Droste, J. J.; Fuson, K. S.; Gitter, B. D.; Hyslop, P. A.;

Johnstone, E. M.; Li, W. Y.; Little, S. P.; Mabry, T. E.; Miller, F. D.; Audia, J. E. *J Neurochem* **2001**, 76, 173-81.

12. Geling, A.; Steiner, H.; Willem, M.; Bally-Cuif, L.; Haass, C. *EMBO Rep* **2002**, 3, 688-94.